Available online at www.sciencedirect.com
SCIENCE DIRECT
International Journal of Hydrogen Energy 31 (2005) 379–389
International Journal of HYDROGEN ENERGY
www.elsevier.com/locate/ijhydene

A hybrid model of cathode of PEM fuel cell using the interdigitated gas distributor

Xun-Liang Liu, Ya-Wei Tan, Wen-Quan Tao*, Ya-Ling He

State Key Laboratory of Multiphase Flow in Power Engineering, Xi'an Jiaotong University, Xi'an 710049, China

Available online 20 December 2005

Abstract

A two-dimensional (2D), single- and two-phase, hybrid multi-component transport model is developed for the cathode of PEM fuel cell using interdigitated gas distributor. The continuity equation and Darcy's law are used to describe the flow of the reactant gas and production water. The production water is treated as vapor when the current density is small, and as two-phase while the current density is greater than the critical current density. The advection–diffusion equations are utilized to study species transport of multi-component mixture gas. The Butler–Volmer equation is prescribed for the domain in the catalyst layer. The predicted results of the hybrid model agree well with the available experimental data. The model is used to investigate the effects of operating conditions and the cathode structure parameters on the performance of the PEM fuel cell. It is observed that liquid water appears originally in the cathodic catalyst layer over outlet channel under intermediate current and tends to be distributed uniformly by the capillary force with the increase of the current. It is found that reduction of the width of outlet channel can enhance the performance of PEM fuel cell via the increase of the current density over this region, which has, seemingly, not been discussed in previous literatures.

Keywords: PEM; Fuel cell; Interdigitated gas distributor; Numerical model

1. Introduction

Fuel cells convert electrochemical energy directly to electrical energy with much less pollution and much better conversion efficiency. There are many different types of fuel cells, among whom the proton-exchange-membrane (PEM) fuel cell is considered as a strong alternative power source for future automobiles. It is also a promising candidate for portable electronic appliance, fixed power generations and distributed power systems.

However, the performance of the PEM fuel cells is limited by the slow kinetic rate of the oxygen and mass transport resistance imposed by the liquid water in the cathode, especially when the air is used as an oxidant. The excessive water, generated by the electrochemical reaction and electro-osmotic drag, could even submerge the catalyst particle, resulting in great reduction of the effective reaction surface, which severely deteriorates the performance of fuel cells. In 1996, a new gas distributor called the interdigitated gas distributor was proposed by Nguyen [1], and it has been proven to be very effective in enhancing the transport of the reactant gases to the reactive sites and reducing the electrode flooding in the cathode. The increase in performance is ascribed to the conversion of species transport from the diffusion mechanism to the convective mechanism in the gas diffusion layer and fast water removal from the cathode catalyst layer.

* Corresponding author. Tel./fax: +86 29 82669106.
E-mail address: wqtao@mail.xjtu.edu.cn (W.-Q. Tao).

0360-3199/$30.00
doi:10.1016/j.ijhydene.2005.11.009

Nomenclature

A_V	specific area of the electrode, $cm^2\,cm^{-3}$
c	molar concentration, $mol\,cm^{-3}$
D	mass diffusivity, $cm^2\,s^{-1}$
F	Faraday constant, $96\,487\,C\,mol^{-1}$
H	electrode height, cm
j	current density, $A\,cm^{-2}$
j_0	exchange current density, $A\,cm^{-2}$
J	mass flux of species, $mol\,cm^2\,s^{-1}$
k_{rg}	relative permeability of gas phase
k_{rlw}	relative permeability of liquid phase
K	permeability of electrode, cm^2
L_1	half of inlet channel width, cm
L_2	half of outlet channel width, cm
L	total width of cathode, cm
p	pressure, atm
r_w	mass transfer rate of water between two phases
R	universal gas constant, $8.3145\,J\,mol^{-1}\,K^{-1}$
R_m	ohmic resistance of membrane, $\Omega\,cm^2$
s	saturation of liquid phase
S^*	normalized saturation
T	temperature, K
$\mathbf{u}$	velocity vector, $cm\,s^{-1}$
v	velocity components in y-direction, $cm\,s^{-1}$
V	electrical potential, V
w	mass fraction of species
x	coordinate, cm
y	coordinate, cm
z	electron number of electrochemical reaction

Greek letters

α	transfer coefficient of electrochemical reaction
β	net water transport coefficient per proton
ε	dry porosity of electrode
ρ	density ($kg\,cm^{-3}$)
η	overpotential (V)
μ	viscosity ($kg\,cm^{-1}\,s^{-1}$)
σ	surface tension ($N\,cm^{-1}$)

Subscripts

av	average
a	anode
c	cathode/capillary
eff	effective
g	gas
i	species
in	inlet channel
ir	irreducible
lw	liquid water
o	oxygen
oc	open circuit
out	outlet channel
ref	reference values
sat	saturation condition
w	water

Recently, there have been some studies on modeling the reactant and production transport in the cathode of PEM fuel cell using the interdigitated gas distributor. Yi and Nguyen [2] proposed a two-dimensional (2D) steady-state multi-component transport model for the porous electrode and investigated the effects of the operating conditions and design parameters of an air cathode on the performance of the cell with an interdigitated gas distributor. Kazim and Liu [3] developed a simple 2D mathematical model to study the superiority of this new kind of distributor design over the conventional one and their modeling results show good performance of the former. He et al. [4] developed a 2D, two-phase multi-component transport model to investigate the effects of the gas and liquid water hydrodynamics on the performance of an air cathode of a PEM fuel cell using an interdigitated gas distributor and investigated the effects of the operating conditions and design parameters of an air cathode on the performance of the cell. Wang et al. [5] investigated the effects of magnet particles on the performance of a PEM fuel cell with an interdigitated gas distributor using a 2D, two-phase transport model similar to the one developed by He et al. Zhou and Liu [6] studied the enhancement of heat transfer in fuel cells with interdigitated flow field design using a 3D single-phase computational model. Natarajan and Nguyen [7] expanded a 2D model for conventional gas distributors to account for the dimensional effect along the length of channel. It is worth noting that there are few two-phase models, and the only two models we found are that of He et al. [4] and Wang et al. [5]. In their works the permeability and capillary driving force functionalities were grouped together and expressed via the interfacial drag coefficient and a capillary diffusion coefficient, which were assumed constants for the sake of simplicity.

In this paper, a 2D, single- and two-phase, steady-state, isothermal, hybrid multi-component transport model is developed for the cathode of PEM fuel cell using interdigitated gas distributor. The continuity equation and Darcy's law are used to describe the flow of the reactant gas and production water. The production water is treated as either vapor or two-phase according to the magnitude of current density and the water transport equations as well as the boundary conditions are different accordingly. An empirical relation is used as the permeability function to depict the dependence on saturation and the Leverett's function is used for capillary force. The model is used to simulate the transport of the species and to investigate the effects of operating conditions and the cathode structure parameters on the performance of the PEM fuel cell.

In the following, the physical and mathematical models are first described in detail, including the solution domain, governing equations and boundary conditions, then the model is applied to a specific PEM fuel cell. The simulated results are compared with available test data, showing good agreement between simulation and test results. The model is then used to study the effects of some geometric and operational conditions, and the simulation results are discussed in detail. Finally, major conclusions are summarized from this study.

2. Model description

The computational domain consists of the gas diffusion layer and catalyst layer of the cathode of MEA as shown in Fig. 1 by the region surrounded by the dashed. The domain includes a half of inlet channel denoted by (1) in Fig. 1(b), a half of outlet channel (2) and a shoulder (3). Normally, the operating temperature of PEM fuel cell is below 100 °C and the system operation pressure is around one atmosphere, hence the water generated by electrochemical reaction and transported by electro-osmotic drag can be considered as liquid phase in the catalyst layer. However, when the current density is small, the liquid water will be evaporated immediately after its generation because the dry air is usually used as the oxygen reactant and the mass faction of water vapor of the air is far-below saturation. In such case the water is present as vapor. In the diffusion layer, the water vapor is transported from catalyst layer (4) to the outlet channel through the flow of mixture gas driven by the pressure difference. While for the case of high current density, water is present in liquid state. The water removal from the electrode is driven by two mechanisms: capillary force driven by saturation gradient and interfacial shear force imposed on by gas flow. The presence of liquid water has an important influence on the performance of the fuel cell by flooding the active sites of catalyst and cumbering the transport of oxygen to the reactive region. Thus, a good model should be able to distinguish the two regimes of the state of the production water: single phase of vapor or two phase of vapor and liquid.

2.1. Model assumptions

In this study, all phases are assumed to be continuous so that the continuum approach is applicable. The catalyst layer is assumed ultra thin and can be treated as a single reactive interface between membrane and diffusion layer. The gas diffusion layer is treated as an isotropic and homogenous porous medium and the properties such as porosity, tortuosity and the permeability are uniform. The gas mixtures are assumed to be well mixed and can be regarded as the ideal gases. The domain is isothermal and only steady state is considered. The effect of the gravity is neglected. The cathodic overpotential is assumed as a known quantity.

2.2. Governing equations

In general, the transport of the reactant and production water conforms to the mass, momentum, and species conservation principles. The velocities of two phases are estimated by Darcy's law. Thus, the governing equations of the model can be written as the following:

$$\nabla \cdot (\rho_g \mathbf{v}_g) = r_w, \tag{1}$$

$$\nabla \cdot (\rho_{lw} \mathbf{v}_{lw}) = -r_w, \tag{2}$$

$$\mathbf{v}_g = -\frac{K_g}{\mu_g} \nabla p_g, \tag{3}$$

$$\mathbf{v}_{lw} = -\frac{K_{lw}}{\mu_{lw}} \nabla p_{lw}, \tag{4}$$

$$\nabla \cdot (\rho_g \mathbf{v}_g w_o) + \nabla \cdot J_o = 0, \tag{5}$$

$$\nabla \cdot (\rho_g \mathbf{v}_g w_w) + \nabla \cdot J_w = -r_w. \tag{6}$$

In the above equations ρ, $\mathbf{v}$, p, and μ are the density, superficial velocity, pressure, and the viscosity of the fluid, respectively; K is the permeability in the porous electrode, and the subscripts 'g' and 'lw' denote gas phase and liquid water, respectively. The symbols of w_o and w_w are the mass fraction

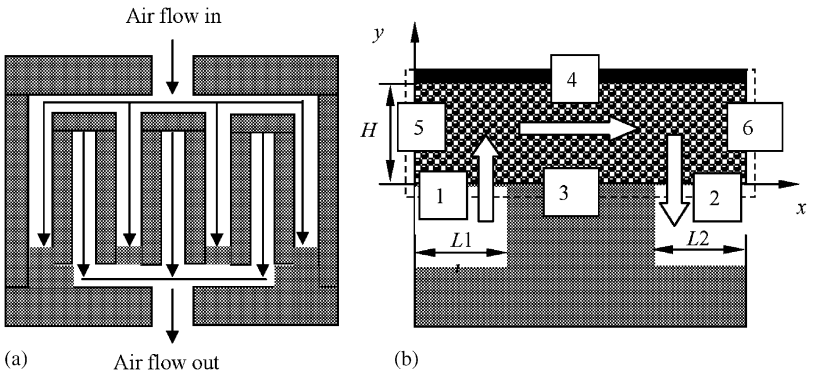

Fig. 1. Schematic of the cathode using the interdigitated gas distributor: (a) top view and (b) cross-sectional view.

of the oxygen and water vapor in the gas mixtures, and J_o and J_w are the mass flux of the oxygen and the water vapor, respectively. The term r_w is the mass transport rate of water between the gas and liquid phase. When the current density is very small, it is treated as zero, and when the current density is increased this term is determined as follows:

$$r_w = h_m A_V \varepsilon s(\rho_g w_{wsat} - \rho_g w_w), \tag{7}$$

where h_m is the mass transfer coefficient of water treated as a constant for simplicity, A_V is the specific area per unit volume of the porous medium, ε is the dry porosity of the diffusion layer, s is the saturation of liquid water indicating the fraction of the void volume occupied by liquid phase in the porous electrode, and w_{wsat} is the mass fraction of vapor in the gas mixtures corresponding to saturation at the operating temperature. Since the fuel cell is assumed isothermal in this work, the condensation of water vapor is not taken into account.

The pressure of liquid water is related with the gas pressure by

$$p_c = p_g - p_{lw}, \tag{8}$$

where p_c is named capillary pressure and is assumed to be a function of liquid water saturation s. The empirical model for the relation between p_c and s is written as [8]

$$F(s) = \frac{p_c}{\sigma}\sqrt{\frac{K}{\varepsilon}}, \tag{9}$$

$$F(s) = 1.417(1 - S^*) - 2.120(1 - S^*)^2 + 1.263(1 - S^*)^3, \tag{10}$$

where $F(s)$ is the Leverett's function, σ is the surface tension for the interface between two phases, and S^* is the normalized saturation, defined as

$$S^* = \frac{s - s_{ir}}{1 - s_{ir}}, \tag{11}$$

where s_{ir} is the irreducible saturation and is set to zero in this paper for simplicity.

The permeability for the liquid and gas phases is represented by

$$K_g = K \cdot k_{rg}, \tag{12a}$$

$$K_w = K \cdot k_{rlw}, \tag{12b}$$

where k_{rg} and k_{rlw} are the relative permeability for the gas and liquid phases, respectively. They are assumed to be the cubic function dependent on the relative saturation [9]

$$k_{rg} = (1 - S^*)^3, \tag{13a}$$

$$k_{rlw} = S^{*3}. \tag{13b}$$

Thus, the governing equations for the gas pressure and liquid saturation can be induced and re-arranged through the substitution to the governing equations (1)–(4) with above Eqs. (8)–(13). Their final formulations are as follows:

$$\nabla \cdot \left(\frac{\rho_g K k_g}{\mu_g} \nabla p_g \right) = r_w, \tag{14}$$

$$\nabla \cdot \left(\rho_{lw} \frac{\mu_g}{\mu_{lw}} \frac{k_{rlw}}{k_{rg}} \mathbf{v}_g \right) + \nabla \cdot \left(\rho_{lw} \frac{K k_{rlw}}{\mu_{lw}} \frac{\partial p_c}{\partial s} \nabla s \right) = 0. \tag{15}$$

The density of gas mixtures is estimated by the ideal gas law

$$\rho_g = \frac{M_g p_g}{RT}, \tag{16}$$

where M_g is the molecular weight of gas mixtures, R is the general gas constant, and T is the operating temperature.

The diffusive flux is obtained by the first Fick's law

$$J_i = -\rho D_{i,\text{eff}} \nabla w_i. \tag{17}$$

The effective mass diffusion coefficient $D_{i,\text{eff}}$ in the porous medium is estimated with a Bruggeman-type relationship

$$D_{i,\text{eff}} = D_i \varepsilon_g^{1.5}, \tag{18}$$

where D_i is the diffusion coefficient of gas species in a nonporous system, and ε_g is the gas porosity which is defined as $\varepsilon_g = \varepsilon(1-s)$. D_i is related with the diffusion coefficient under the reference condition expressed by

$$D_i = D_{i,\text{ref}} \left(\frac{T}{T_{\text{ref}}}\right)^{1.5} \left(\frac{p}{p_{\text{ref}}}\right)^{-1}, \tag{19}$$

where $D_{i,\text{ref}}$ is the referenced value of diffusion coefficient at $T_{\text{ref}} = 25\,^{\circ}\text{C}$ and $p_{\text{ref}} = 1.013 \times 10^5$ Pa.

2.3. Boundary conditions

The modeled region has six distinct boundaries. At the inlet, namely the interface between the channel and the diffusion layer (Boundary 1 in Fig. 1(b)), the gas pressure and the mass fraction of each species are specified as

$$p_g = p_{\text{in}}, \quad w_o = 0.21, \quad w_w = 0. \tag{20}$$

For the equation of liquid saturation, Eq. (15), no flux of liquid water is set as the inlet boundary condition, which means that the y-directional liquid water velocity is equal to zero

$$v_{\text{lw}} = 0. \tag{21}$$

At the outlet (Boundary 2), the gas pressure is specified, and change rates in the mass fractions and the saturation are assumed to be zero. Thus, the outlet boundary conditions are set as follows:

$$p_g = p_{\text{out}}, \quad \frac{\partial w_o}{\partial y} = 0, \quad \frac{\partial w_w}{\partial y} = 0, \quad \frac{\partial s}{\partial y} = 0. \tag{22}$$

At the interface between the shoulder of the distributor and the electrode (Boundary 3), nonpermeability condition is used for this boundary:

$$\frac{\partial p_g}{\partial y} = 0, \quad \frac{\partial w_o}{\partial y} = 0, \quad \frac{\partial w_w}{\partial y} = 0, \quad \frac{\partial s}{\partial y} = 0. \tag{23}$$

At the Boundaries 5 and 6 shown in Fig. 1(b), symmetry conditions are used

$$\frac{\partial p_g}{\partial x} = 0, \quad \frac{\partial w_o}{\partial x} = 0, \quad \frac{\partial w_w}{\partial x} = 0, \quad \frac{\partial s}{\partial x} = 0. \tag{24}$$

Boundary 4 is the interface between the electrode and the membrane. Since the membrane is not permeable for the gas, the y-directional superficial velocity of gas mixtures is assumed to be zero. In addition, the interface is the domain for the electrochemical reaction where the oxygen is depleted and the water is generated by reaction and accumulated due to mass transport by the electro-osmosis drag from the anode side. When the current density is small, the water is present as vapor and the studied fluid is single phase. Hence, the saturation equation needs not to be solved and the saturation is set equal to zero for whole computational domain. For this situation, the boundary conditions can be determined as follows:

$$\frac{\partial p_g}{\partial y} = 0, \quad J_o = \frac{j}{4F}, \quad J_w = -\left(\frac{1}{2} + \beta\right)\frac{j}{F}, \tag{25a}$$

where j is the local current density at the interface, F is the Faraday's constant, and β is the ratio of the net water transport rate across the membrane per proton by the electro-osmotic drag.

When the current density is larger than the critical value and air is over-saturated with vapor, two-phase flow should be considered and the water saturation equation (Eq. (15)) should be coupled with other governing equations. And the following equations are used as the conditions at Boundary 4:

$$\frac{\partial p_g}{\partial y} = 0, \quad J_o = \frac{j}{4F},$$

$$J_w = -\left(\frac{1}{2} + \beta\right)\frac{j}{F}, \quad \frac{\partial s}{\partial y} = 0. \tag{25b}$$

The local current density distribution is obtained by the Bulter–Volmer equation modified by the term considering the liquid water flooding the active reaction sites [10]

$$j = j_0 \frac{c_o(1-s)}{c_{o,\text{ref}}} \exp\left(\frac{\alpha z F}{RT}\eta_c\right), \tag{26}$$

where j_0 is the exchange current density, η_c is the cathodic overpotential, c_o is the molar concentration of oxygen, $c_{o,\text{ref}}$ is the reference concentration, α is the cathodic transfer coefficient, and z is the reactive electron number.

Table 1
Values for parameters used in the base case

Parameter	Value
Electrode height	0.00025 m
Inlet channel width	0.0005 m
Outlet channel width	0.0005 m
Shoulder width	0.001 m
Permeability of the electrode	$1.2 \times 10^{-12}\ m^2$
Dry porosity of the electrode	0.3
Mass fraction of oxygen at inlet	0.21
Mass fraction of vapor at inlet	0
Inlet gas pressure	1.01 atm
Outlet gas pressure	1 atm
Operating temperature	60 °C
Viscosity of air (60 °C)	$2.03 \times 10^{-5}\ kg\ m^{-1}\ s^{-1}$
Reference diffusivity of oxygen	$0.1775 \times 10^{-4}\ m^2\ s^{-1}$ (1 atm, 0 °C)
Reference diffusivity of water	$0.256 \times 10^{-4}\ m^2\ s^{-1}$ (1 atm, 34 °C)
Exchange current density	$100\ A\ m^{-2}$
Electron number of electrochemical reaction	4
Membrane resistance [11]	$0.285 \times 10^{-4}\ \Omega\ m^2$
Transfer coefficient of electrochemical reaction	0.5
Net water transport coefficient of membrane	0.5
Water mass transfer coefficient [12]	$0.016\ m\ s^{-1}$
Specificarea of the electrode	$1 \times 10^{-5}\ m^{-1}$
Surface tension [13]	$0.0625\ N\ m^{-1}$
Open-circuit voltage	1.0 V
Cathodic overpotential	0.25 V

The average current density is estimated by integrating the local current densities generated along the reactive interface

$$j_{av} = \frac{1}{L}\int_0^L j(x)\,dx. \tag{27}$$

By neglecting the anodic overpotential, the electrical potential of the fuel cell is calculated as

$$V_{cell} = V_{oc} - \eta_c - j_{av}R_m, \tag{28}$$

where V_{oc} is the open-circuit voltage of the cell and R_m is the Ohmic resistance in the membrane.

2.4. Model solutions

The governing equations, Eqs. (5), (6), (14), and (15), together with the boundary conditions are solved numerically by a finite-volume method. Firstly, the gas pressure and gas velocity fields are obtained by solving pressure equation. Then the mass fractions of gas species and liquid saturation equations are solved, which are dependent on the current density. As indicated above, the cathodic overpotential is assumed as a known quantity, then the local current densities can be calculated and the coupled transport equations are solved iteratively for the other unknowns. The solution is considered to be convergent when the relative deviation in each dependent variable between two consecutive iterations is less than 10^{-5}.

As indicated above, when the current density is small, the water is present as vapor and the studied fluid is single phase. Hence the water saturation is set equal to zero for whole model domain. As the current density is increased, gas mixtures are humidified and saturated, then liquid water is present and Eq. (15) should be solved with related boundary conditions. That is the reason why the present method is called hybrid model.

During the solution procedures of a systematic study in which the current density varies within a wide range, the vapor mass fraction of the whole computational domain is checked regularly to find whether the maximum value is greater than the saturation value. If it is, the two-phase model should be used and the liquid water saturation equation should be solved for the whole computational domain. For the case studied (Table 1) the critical current density is obtained about $0.4\ A/cm^2$, at which the numerical result of the maximum mass fraction of the water vapor reaches its saturated value. Fortunately, a little liquid water flooding can be captured by the numerical simulation. For instance, if the

inlet humidity is low and the first part of the GDL is in single-phase regime, but at certain point along the GDL the gas stream becomes saturated due to water production and electro-osmosis, and liquid water may be present, then the result of the regular check of the vapor mass fraction will switch the single-phase model into the two-phase one.

The above model is first applied to a specific fuel cell for which the geometric and operation conditions are listed in Table 1. Some comparison is made for the potential vs. current density relation from the experimental data and the numerical results to demonstrate the validity of the present model. The velocity fields of gas mixture and liquid water are presented, followed by the introduction of water saturation distribution and water vapor mass fraction profile. The model is then used to study the effects of operating pressure and the inlet/outlet channel width ratio on the fuel cell performance. The numerical results are presented as follows.

3. Results and discussion

3.1. Model validation

The present model is applied to the fuel cell studied in [4] and the predicted polarization curve is compared with the experimental data in Fig. 2. Also the numerical results from the single-phase model is shown in the figure for comparison purpose. As it can be seen from the figure, a better agreement is achieved by the hybrid model than by the single-phase model because the excessive water flooding of the cathode is taken into account in the hybrid model. The water saturation equation needs not be solved when the current density is less than the critical value, the solution process of hybrid model is time-saving compared with that of the two-phase model [4]. While the current density is larger than the critical value, its solution procedure is the same as that of two-phase model.

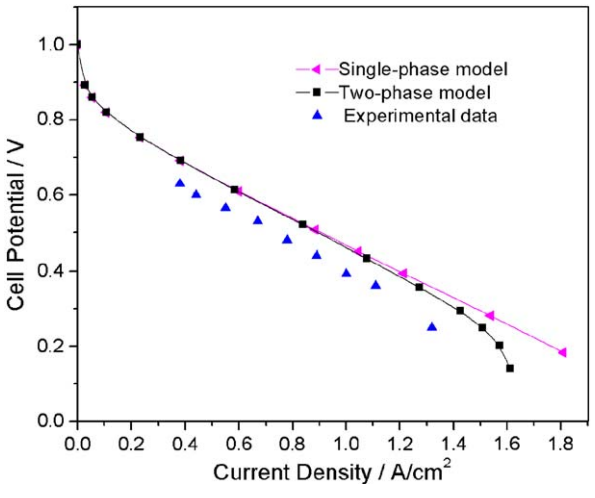

Fig. 2. Model prediction of the polarization curve and experimental data.

The small discrepancy between the hybrid model prediction and experimental data may be due to the neglect of anodic overpotential. It should be noted that the experimental data for small current density were not available in [4]. The figure shows that the cell potential drops dramatically at low current densities. The activation polarization is mainly responsible for the potential losses in this region. At higher current densities, the curve is linear resulted from the Ohmic resistance of membrane. When the current density is approaching the value of 1.4 A cm^{-2}, the cathodic polarization is gradually limited by the mass transport of oxygen and the water flooding of catalyst layer, and the polarization curve becomes nonlinear again in the region of larger current density.

Fig. 3 shows the velocity field of gas mixture and Fig. 4 presents the velocity field of liquid water for the base case shown in Table 1. It can be clearly observed that the larger gas velocities are located at the inlet/shoulder and outlet/shoulder corners because the flow is induced by the pressure driving force. At the electrode/membrane interface, the gas velocity is low and the diffusion mechanism is predominant. The liquid water velocity is small in the region over inlet and left/right symmetric boundaries (Boundaries 5, 6), and much larger near the outlet/shoulder corner. It can be ascribed to the fact that water is generated at the electrode/membrane interface and transferred by capillary diffusion and shear force existing in the gas flow. Our numerical results shows that the maximum of gas velocity is about 6 cm s^{-1} and the liquid velocity is at least three orders of magnitude smaller than that of the gas mixtures.

Fig. 5 displays the liquid water saturation distributions under different operating current density. When the current is just a bit more than the critical current, liquid water appears in the downstream of electrode and the maximum saturation value is located in the corner over the outlet (Fig. 5(a)). With the increase of current density, more liquid water is produced by the electrochemical reaction and electroosmosis and distributed almost uniformly (ranged from 10% to 14%) in the whole electrode (Fig. 5(c)). From Fig. 5(a)–(c), following common feature maybe noted. The saturation value has a minimum near the inlet/shoulder corner because there

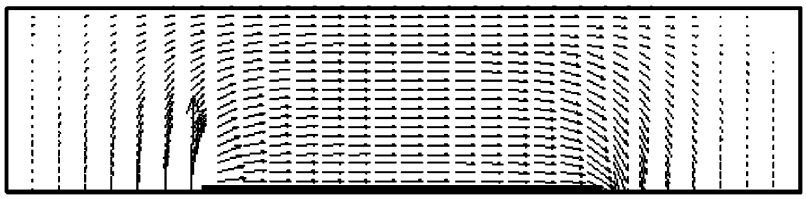

Fig. 3. The velocity field of gas mixture for the base case.

Fig. 4. The velocity field of liquid water for the base case.

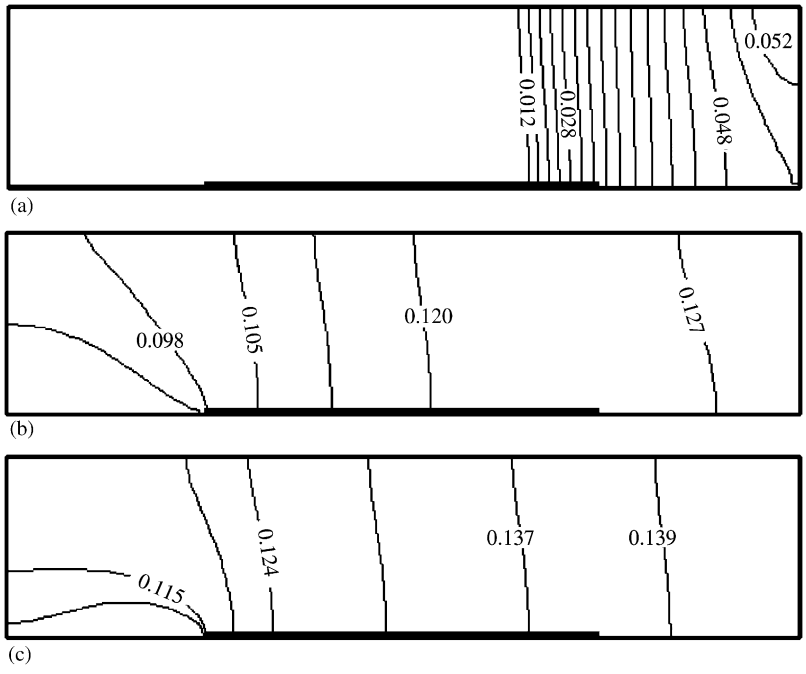

Fig. 5. The liquid water saturation distribution (a) $I_{av} = 0.6\,A\,cm^{-2}$, (b) $I_{av} = 1.2\,A\,cm^{-2}$ and (c) $I_{av} = 1.4\,A\,cm^{-2}$.

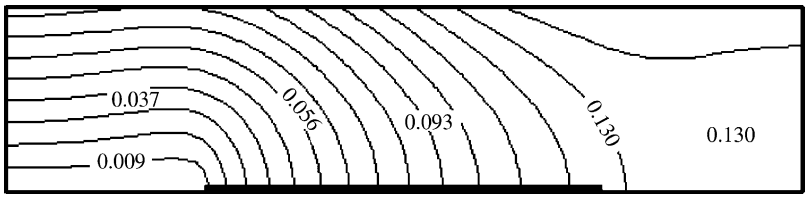

Fig. 6. The vapor mass fraction profile for the base case.

is the maximum of the gas flow shear force, and there is a gradually increasing trend of water saturation in the downstream direction through the electrode.

As the dry air flows transversely across the electrode, it is humidified by the water produced and transported from anode and at downstream side it may be saturated or over-saturated with vapor (vapor saturation mass fraction is about 13%), as shown in Fig. 6. This leads to a smaller water saturation distribution at upstream side and a larger saturation located at the electrode/membrane corner of downstream side, where the capillary force driven by saturation gradient is small and the shear force by gas flow is approximately equal to zero. The distribution discovered in our numerical simulation is quite different from other works [4,5], which gained a larger saturation gradient and un-uniform water saturation distribution in the cathode. This is probably ascribed to the different ways of achieving the capillary diffusion coefficient.

3.2. Study on the effects of the operation pressure and inlet/outlet channel width ratio

The effects of some operating parameters on fuel cell performance are investigated with this model. These include the pressure drop between inlet and outlet channels, electrode height, the number of channels with the total reactive area remained the same, the width of shoulder, the operation pressure and the width ratio of inlet and outlet channels. The results show that a higher pressure drop between inlet and outlet channels, more channels and shorter shoulder widths all can improve the performance and the electrode height needs to be optimized to get optimal performance. These conclusions are similar to that obtained in the previous works [2,4]. So they are not to be depicted in detail for brevity, only Figs. 7 and 8 are shown to present our numerical results of inlet pressure effect. Fig. 8 shows that the local current density in the region near the outlet channel is much lower than that near the inlet channel. This is mainly owing to the transport limit of oxygen to the catalyst layer over the outlet channel. This observation inspires us to conduct further study for improving the performance of cell. One simple way to enhance the transport process in the outlet channels is to increase the gas velocity there and this can be realized by reduction the outlet channel width. In the following the numerical results of the effect on cell performance of width ratio between inlet/outlet channels are presented, which are seldom discussed in the previous literatures.

As shown in Fig. 9, increasing the ratio between inlet and outlet channel width by decreasing the outlet channel width is in favor of enhancing the performance of cell with other parameters of the electrode unchanged. The local current density profiles along the electrode for different outlet channel widths are shown in Fig. 10. As indicated above narrow outlet channel can increase the gas velocity in the channels and more oxygen is transported to the electrode/membrane interface. In addition, the produced water can be removed more quickly. Thus the local current density is improved in this region. Moreover, there is a very small decrease the current density in the region over the inlet channel. So the average current density along the electrode increases and the fuel cell can operate in a larger range of current density. It is a simple and practical method for improving the fuel cell performance by small change of distributor geometric design. Our numerical finding

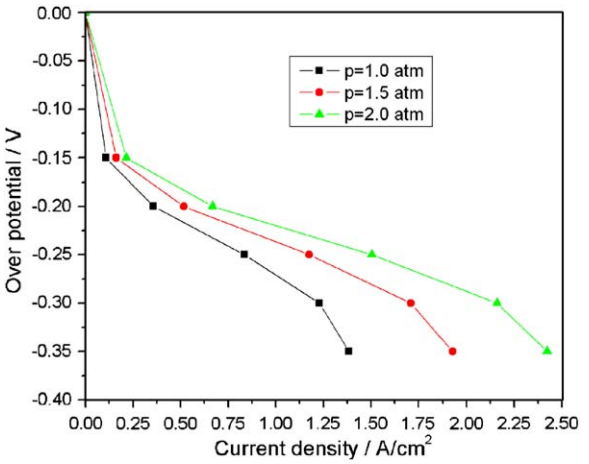

Fig. 7. Effect of operating pressure on the cell performance.

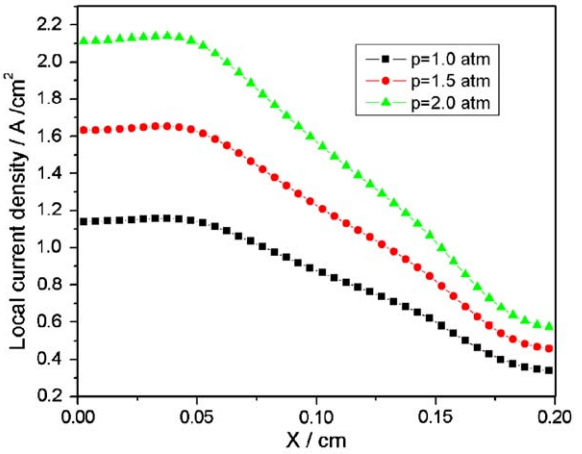

Fig. 8. Effect of operating pressure on the local current density profiles along the cathode width.

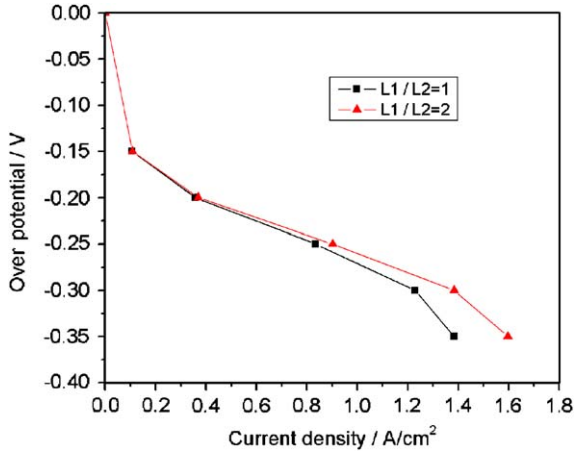

Fig. 9. Effect of increasing the ratio between inlet and outlet channel widths on the cell performance.

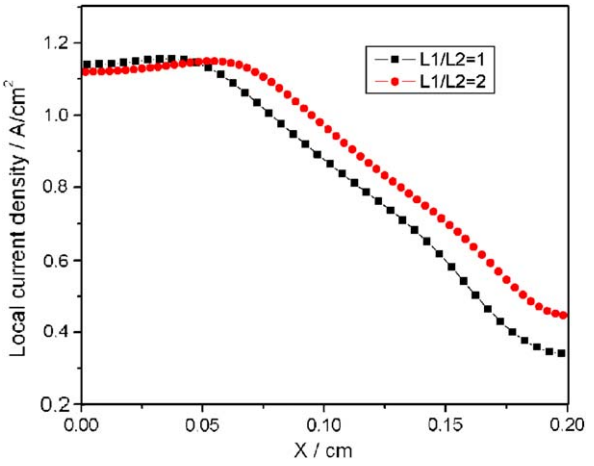

Fig. 10. Effect of increasing the ratio between inlet and outlet channel widths on the local current density profiles along the cathode width.

is consistent with the experimental results performed in [14].

4. Conclusions

In the article, a 2D, single- and two-phase, hybrid multi-component transport model is developed for cathode of PEM fuel cell using the interdigitated gas distributor. The continuity equation and Darcy's law are used to describe the flow of the reactant gas and production water. The production water is treated with one- or two-phase according to the magnitude of current density, and the corresponding transport equations along with the appropriate boundary conditions are adopted. An empirical relation is used as the permeability function to depict the dependence on saturation and the Leverett's function is used for capillary force. The model is validated by comparison between the simulated results and available experimental data, and good agreement is achieved. The proposed model is used to investigate the flow field and saturation distribution of liquid water, and the effects of some parameters on the performance of the fuel cell are studied. The major findings of this paper can be summarized as follows:

(1) The liquid water flows towards the outlet channel in the cathodic diffusion layer and its velocity is at least three orders of magnitude smaller than that of the gas mixtures.
(2) Liquid water appears originally in the cathodic catalyst layer over outlet channel under intermediate current density. While increasing the operating current, liquid water tends to be distributed uniformly by the capillary force.
(3) Reduction of the outlet channel width is in favor of enhancing the cell performance by increasing the oxygen transport rate and water removal rate in the downstream region.

Acknowledgements

This work was supported by the National Natural Science Foundation of China under Grant No. 50236010.

References

[1] Nguyen TV. A gas distributor design for proton-exchange-membrane fuel cells. J Electrochem Soc 1996;143:L103–5.
[2] Yi JS, Nguyen TV. Multicomponent transport in porous electrodes of proton exchange membrane fuel cells using the interdigitated gas distributors. J Electrochem Soc 1999;146:38–45.
[3] Kazim A, Liu HT. Modeling of performance of PEM fuel cells with conventional and interdigitated flow fields. J Appl Electrochem 1999;29:1409–16.
[4] He W, Yi JS, Nguyen TV. Two-phase flow model of the cathode of PEM fuel cells using interdigitated flow fields. AIChE J 2000;46:2053–64.
[5] Wang LB, Wakayama NI, Okada T. Numerical simulation of a new water management for PEM fuel cell using magnet particles deposited in the cathode side catalyst layer. Electrochem Commun 2002;4:584–8.
[6] Zhou T, Liu H. Heat transfer enhancement in fuel cells with interdigitated flow field design. Prog Comput Fluid Dynamics 2002;2:97–105.
[7] Natarajan D, Nguyen TV. Three-dimensional effects of liquid water flooding in the cathode of a PEM fuel cell. J Power Sources 2003;115:66–80.

[8] Leverett MC. Capillary behavior in porous solids. Trans AIME 1941;142:152–69.
[9] Kaviany M. Principles of heat transfer in porous media. New York: Springer; 1991.
[10] Natarajan D, Nguyen TV. A two-dimensional two-phase multicomponent transient model for the cathode of aproton exchange membrane fuel cell using conventional gas distributors. J Electrochem Soc 2001;148(12):A1324–1335.
[11] Vafai K. Handbook of porous media. New York: Marcel Dekker; 2000.
[12] Springer TE, Zawodzinski TA, Gottesfeld S. Polymer electrolyte fuel cell model. J Electrochem Soc 1991;138:2334–42.
[13] Wang ZH, Wang CY, Chen KS. Two-phase flow and transport in the air cathode of proton exchange membrane fuel cells. J Power Sources 2000;4094:40–50.
[14] H. Guo, Study of polar plate and its flow bed of proton exchange membrane direct methanol fuel cells. Phd thesis, Xi'an Jiaotong University, Xi'an, China, 2004.